26th EPS Conf. on Contr. Fusion and Plasma Physics, Maastricht, 14 - 18 June 1999 ECA Vol.23J (1999) 441 - 444

Construction, operational scenarios, and research plan of TST-2

S. Shiraiwa, Y. Takase, A. Ejiri, K, Yamagishi,
Y. Nagashima, N. Kasuya
Department of Physics, Graduate School of Science, University of Tokyo
Hongo 7-3-1, Bunkyo-ku, Tokyo, 113-0033, Japan

1. Introduction

The spherical tokamak (ST) has attracted growing attention since Peng and Strickler predicted its potential advantages in 1986.[1] These advantages include high plasma current capability at low toroidal field, high toroidal beta, high natural elongation, and nearly omnigeneous region in the bad curvature region. Experimentally, START (Small Tight Aspect Ratio Tokamak)[2,3] has demonstrated these promising features of the spherical tokamak, and has recently succeeded in sustaining a high beta (40%) plasma.[4] These encouraging results are being followed by the new generation of STs such as MAST[5], NSTX[6], GLOBUS-M[7], and PEGASUS.[8]

Tokyo Spherical Tokamak (TST) and TST-M have explored the possibility of helicity injection current drive[9] and studied turbulence-induced transport.[10] The magnetic fluctuation decreased as the aspect ratio decreased from A=2.5 (conventional tokamak) to A = 1.4 (ST). It was shown that the contribution of magnetic turbulence was less than 2% of the total electron heat transport estimated from global power balance. However, these results were obtained for relatively low density (several $10^{18}m^{-3}$) and low temperature (several tens of eV) plasmas.

In order to explore higher temperature and higher density regimes, TST-2[11] has been constructed. The increased OH solenoid volt-second capability and increased toroidal field enable production of plasmas with plasma currents of 0.2-0.4 MA and discharge duration of 50 -100 ms. The discharge "flat-top" will be several times the energy confinement time, which is preferable for transport studies. Additionally, radio-frequency (RF) heating experiments are planned. The comparison of parameters between TST-2 and TST-M is shown in Table 1.

This paper presents the design, expected plasma performance, operational scenarios, and research plans of TST-2.

	TST-M	TST-2 (with Upgrade)
Height of V.V.	1.6m	1.5m
Radius of V.V.	0.9m	0.7m
V.V Wall Thickness	15-20mm	6mm
Toroidal Field	0.2-0.3T	0.2-0.4T
OH Volt-Second	25mVs	130mVs(260mVs)
Major Radius	0.38m	0.37m
Minor Radius	0.28m	0.23m
Aspect Ratio	2.5-1.3	1.6
Elongation	1.0 -1.5	1.2 -1.8
Plasma Current	< 60kA (<150kA transiently)	200kA (400kA)
Discharge Duration	< 10ms	50ms (100ms)

Table 1: Parameter comparison of TST-M (achieved) and TST-2 (expected).

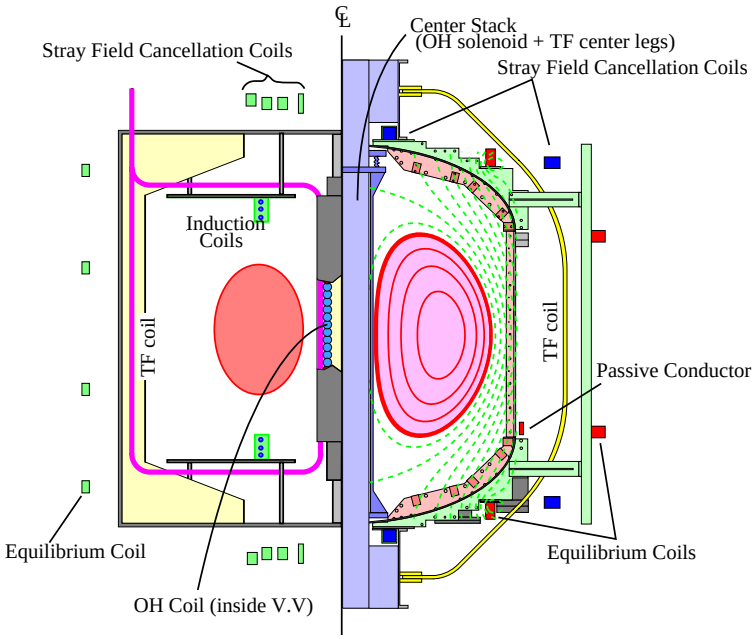

Fig. 1: Cross sections of TST-M (left) and TST-2 (right).

2. Design Features of TST-2

TST-2 has a newly manufactured vacuum vessel that consists of a 1.4m diameter stainless steel cylinder, 0.23m diameter inner wall, and top and bottom semi-elliptic domes. The height of the vacuum vessel is 1.5m. As shown in Fig. 1, the vacuum vessel is similar in size to TST-M. However, as opposed to TST-M, the vessel is continuous in the toroidal direction. In order to reduce the effect of wall-induced eddy currents, the thickness of the vacuum vessel was carefully minimized. The thickness of the cylinder and top and bottom domes is 6mm, while the inner wall is made of a 1.6 mm thick Inconel-625 tube. The top dome and the cylinder are sealed using a Viton O-ring and can be separated for installing large apparatus such as induction coils and RF antennas inside the vessel. The inner and outer limiters are located at R=0.125m and R=0.67m respectively. The plasma major radius is around 0.37m and the minimum possible aspect ratio is 1.5. After installation of the RF heating antenna, this value will be restricted to 1.6.

The new center stack consists of a 239-turn, double-layer ohmic (OH) solenoid and the center legs of the 24-turn toroidal field (TF) coil. The conductors of the center stack are water-cooled. The OH solenoid is designed to provide a flux swing of 130 mVsec for single-swing operation, which is 5 times larger than TST-M. It will be extended to 260 mVsec by using the double-swing mode. The maximum toroidal field capability increases from 0.3T to 0.4T. On TST-M, the OH solenoid and the TF coils were located inside the vacuum vessel. The cross sectional area of the coil conductors were restricted to be relatively small. On TST-2, the position of these coils was moved outside the vacuum vessel. This change results in increased heat capacity and conductivity, which are necessary for extending the discharge duration. The TF capacitor bank is upgraded to meet the increased energy requirement for magnetizing the TF coil.

TST-2 has four pairs of poloidal field (PF) coils. Their roles are cancellation of the ohmic leakage flux, production of the equilibrium field, and creation of the poloidal field null during the breakdown phase. A single-turn passive conductor is located at the symmetric point of the flange. The eddy current induced on the passive conductor will balance the eddy current on the flange, thus making the vacuum magnetic field structure up-down symmetric.

3 Plasma Performance and Experimental Plans

3-1 Plasma Startup

The required loop voltage for discharge startup depends on the prefill pressure and the vacuum magnetic field structure. Since the vacuum vessel of TST-2 is continuous in the toroidal direction, the magnetic field structure must be determined including the effect of eddy currents induced in the vacuum vessel wall. The simulation that we employed treats the vacuum vessel and the poloidal coils as filamentary current rings, calculates the self- and mutual-inductances between current rings, and integrates the differential equations by 4th order Runge-Kutta method.

Figure 2 shows the magnetic field structure at the breakdown phase in the single swing operation. In this mode, one pair of PF coils is connected in series to the OH solenoid and another pair is independently controlled to compensate for the leakage flux of the OH solenoid and the eddy currents. The coil currents are also shown in Fig. 2. A field null appears around R=0.2m on the equatorial plane and the strength of the stray field become less than 1 gauss in a 30cm×50cm region around the field null.

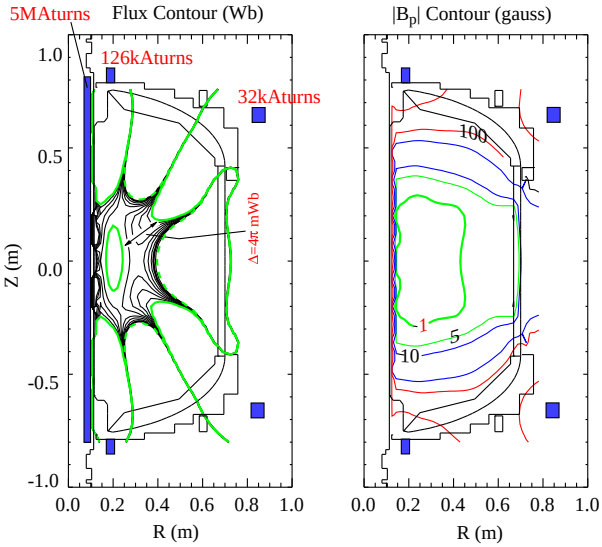

Fig. 2: The flux contour(left) and the strength of stray field (right) at the break down time.

The connection length is more than 1000m and the electric field is about 1.8V/m. The break down time is estimated to be 2-5ms according to the procedure used by Lloyd[12].

3-2 Volt-second Consumption

The volt-second consumption necessary for plasma current build up is the sum of the external flux, the internal flux, and the resistive flux loss. The external flux is estimated using the numerical calculation of Ref.13. The internal flux depends on the internal inductance (l_i) of plasma, while the resistive flux loss is approximated using the Ejima coefficient. The plasma current driven by the OH solenoid is calculated for various l_i (0.3-1.1) and the Ejima coefficient (0.3-0.5). 110mVs is sufficient to drive plasma current of 200kA, leaving 20mVs-50mVs for sustainment. Linearly extrapolating the results obtained on TST-M also shows that a plasma current of 200kA is probable on TST-2.

The necessary loop voltage for the break down and volt-second consumption can be reduced using powerful preionization. On TST-M, electron-cyclotron-resonance heating (ECRH) preionization using 1kW at 2.45GHz was effective for low pressure break down and the maximum plasma current increased by roughly 50%. In addition, empirical scaling shows favorable volt-second consumption efficiency in the ST regime[14].

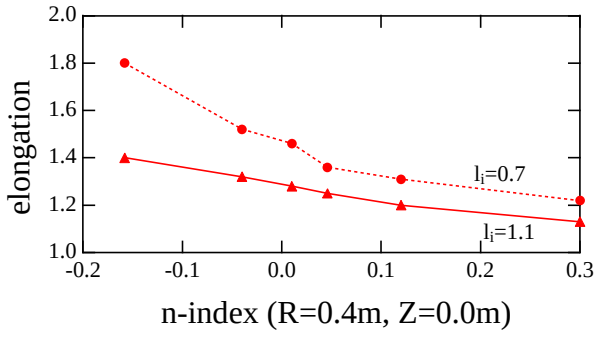

Fig. 3: The plasma elongation vs. curvature of the external magnetic field (n-index).

3-3 Equilibrium

The shape of plasma depends on the structure of the externally applied equilibrium field and the internal inductance. Free boundary MHD equilibrium solution was obtained using the TokaMac[15] code for an aspect ratio A = 1.6 (an example is shown in Fig. 1). The input parameters are : plasma current of 150kA, toroidal field of 0.2T at R=0.4m, central pressure of 2 kPa, and aspect ratio of 1.6. Figure 3 shows the dependence of elongation

(κ=b/a) on curvature of the external magnetic field for two values of internal inductance. Neglecting the MHD stability issue, equilibria of A=1.6 and κ=1.1 ~ 1.8 can be produced on TST-2. At the minimum decay index of Fig. 3, the plasma is marginally stabilized against vertical displacement due to the stabilizing effect of the vacuum vessel. A survey of plasma elongation by reducing the internal inductance down to 0.2 shows that maximum κ is below 2.1. The space above and below the plasma is enough for an abrupt decrease of internal inductance and resultant increase of elongation observed during internal reconnection event (IRE) [5].

It has been shown theoretically and experimentally[16,17] that the edge safety factor limit is more restrictive for ST. Some equilibria shown on Fig. 3 have edge safety factors of 3.5-4.0, and could be near the operational limit.

3-4 Experimental Plans

The goals of TST-2 experiments include turbulence-induced transport and radio-frequency (RF) heating. Transport studies will be continued using Langmuir and magnetic pickup probes. RF physics experiments using the high harmonic fast wave (HHFW) will start at low power (2kW). After research on propagation and absorption properties of HHFW[18], high power plasma heating experiments will start .

4 Summary

In this paper, the design of TST-2, expected plasma performance, operational scenarios, and research plans were described.

A field null will be created at break down by the OH solenoid and the 2 pairs of PF coils. The new OH solenoid can drive a plasma current of 200kA in the single-swing mode of operation. Various MHD equilibria are possible with aspect ratios of A >1.5 and elongations of κ=1.1-1.8.

The manufacturing of the new vessel and the new center stack has completed. Initial vacuum vessel pumping has started and the base pressure is below 5×10^{-8} torr without any wall conditioning. The first plasma is scheduled in the summer of 1999.

References

[1] Y.-K.M. Peng and D.J. Strickler, Nucl. Fusion **26** (1986) 769.
[2] A.Sykes et al., Nucl. Fusion **32** (1994) 769.
[3] D.A.Gates, et al., Phys. Plasmas **5** (1996) 1775.
[4] M. Gryaznevich, et al,. Phys. Rev. Lett. **50** (1998) 3972.
[5] A.C. Darke, et al., in Proc. 18th SOFT (Karlsruhe) (1995) 799.
[6] S. Kaye, et al., Bull. Am. Phys.Soc. **42** (1997) 1988.
[7] V.E.Golant, et al., in Proc. 17th IAEA Fusion Energy Conf., Yokohama, Japan, Oct. 1998, IAEA-CN-69/ICP/02 .
[8] R.J. Fonk, in Proc. IAEA TCM on ST and 4th Int. WS on ST (Tokyo 1998).
[9] H. Toyama, et. al, in Fusion Energy 1996 (Proc. 16th Int. Conf. Montreal 1996) IAEA Vienna (1997) vol.2, 223.
[10] H. Toyama, et al., in Proc. 17th IAEA Fusion Energy Conf., Yokohama, Japan, Oct.19-24, IAEA-CN-69/EXP2/25 (1998).
[11] Y. Takase, A. Ejiri, S. Shiraiwa, Bull. Am. Phys. Soc. **44** (1999) 588.
[12] B. Lloyd, et al., Nuclear Fusion **31** (1991) 2031.
[13] S.P. Hirshman and G.H. Neilson, PhysFluids, **29** (1986) 790.
[14] M. Gryaznevich, in Proc. Int. WS on ST (St.Petersburg 1997).
[15] L. Bai and M. Mauel, Grad-Shafranov solver developed at Columbia University.
[16] M.R. O'Brien, et al., in Fusion Energy 1996 (Proc. 16th Int. Conf. Montreal 1996) IAEA Vienna (1997) vol.2, 57.
[17] M.Ono, et al., in Fusion Energy 1996 (Proc. 16th Int. Conf. Montreal 1996) IAEA Vienna (1997) vol.2, 71.
[18] Y.Takase, et al., in Proc. IAEA TCM on ST and 4th Int. WS on ST (Tokyo Oct. 1998).